

# Engineering the spatial confinement of exciton-polaritons in semiconductors

R. Idrissi Kaitouni,<sup>1</sup> O. El Daïf,<sup>1</sup> M. Richard,<sup>1</sup> P. Lugan,<sup>1,2</sup> A. Baas,<sup>1</sup> T. Guillet,<sup>3</sup>  
F. Morier-Genoud,<sup>1</sup> J. D. Ganière,<sup>1</sup> J. L. Staehli,<sup>1</sup> V. Savona,<sup>2,\*</sup> and B. Deveaud<sup>1</sup>

<sup>1</sup>*Institute of Quantum Electronics and Photonics,*

*Ecole Polytechnique Fédérale de Lausanne EPFL, CH-1015 Lausanne, Switzerland*

<sup>2</sup>*Institute of Theoretical Physics, Ecole Polytechnique Fédérale de Lausanne EPFL, CH-1015 Lausanne, Switzerland*

<sup>3</sup>*Groupe d'Etude des Semiconducteurs (GES), Université de Montpellier II,*

*Place Eugène Bataillon, F-34095 Montpellier, France*

(Dated: July 9, 2021)

We demonstrate the spatial confinement of electronic excitations in a solid state system, within novel artificial structures that can be designed having arbitrary dimensionality and shape. The excitations under study are exciton-polaritons in a planar semiconductor microcavity. They are confined within a micron-sized region through lateral trapping of their photon component. Striking signatures of confined states of lower and upper polaritons are found in angle-resolved light emission spectra, where a discrete energy spectrum and broad angular patterns are present. A theoretical model supports unambiguously our observations.

PACS numbers: 71.36.+c, 71.35.Lk, 42.65.-k

Most of the major advances in semiconductor physics and technology over the last thirty years have been obtained thanks to quantum confinement of elementary excitations along one, two, or three spatial dimensions,[1, 2, 3, 4] and simultaneously to the improvement of their coupling to the electromagnetic field. In this context, quantum dots[3] represent the prototypical system. They are often called “macroatoms”[5] as they allow quasi-zero-dimensional confinement of electronic states and display a discrete spectrum of energy levels. The quantum dot fabrication technique is usually based on a spontaneous formation process producing dots randomly distributed within a restricted range of sizes and shapes.[3] This in turn limits the control over the energy-level structure and makes single-dot applications a challenging task.

As an alternative to electron-hole pairs in quantum dots, confined states of other kinds of excitations in solids can be engineered. To this purpose, two-dimensional polaritons in planar semiconductor microcavities[6, 7, 8] (MCs) are particularly suited. In MCs, the photon part of the polariton is provided by the optical modes of a Fabry-Prot planar semiconductor resonator, which are resonant with the exciton level of an embedded semiconductor quantum well. The dependence of polariton energy on its in-plane momentum has a quadratic behaviour, reminding of a massive particle, with an effective mass typically of the order of  $10^{-5}$  times the free electron mass.[9] It is remarkable that, given this peculiar energy-momentum dispersion, a sizeable spacing of energy levels is expected already when the confinement extends over a few microns – a quite unique situation in a semiconductor artificial structure that makes fabrication, positioning and optical addressing much easier than for other nanostructured systems. Owing to their peculiar nature of weakly interacting bosonic quasiparticles, confined polaritons would be an optimal system for

a wide range of fundamental and applied studies. Polariton parametric processes[11, 12] could be exploited for producing confined polaritons in quantum states displaying nonclassical properties like quantum correlations and entanglement[13, 14]. This, joined to the ease of integration, optical manipulation and readout, could be the premise for a novel kind of quantum information device. Moreover, the discrete spectrum is the key feature[15] to overcome the effect of quantum fluctuations that dominate a two-dimensional interacting Bose gas, and opens the way to the observation of collective many-body effects and long-range order.[16, 17] In a very recent work,[18] we have described a new paradigm of devices that should be able of producing laterally confined polariton states in a MC. A spectroscopical analysis has revealed a series of sharp emission lines that display avoided level crossing when varying the exciton-cavity detuning. In spite of this promising premise, however, a direct experimental evidence of the simultaneous spatial confinement of upper and lower polariton modes is still needed.

In this Letter we present conclusive direct evidence of polariton spatial confinement in a three-dimensional trap. The analysis is carried out by means of angle-resolved photoluminescence (PL) spectroscopy of both confined and extended polariton modes, and is supported by a theoretical model of the polariton states. The new technique for polariton lateral confinement consists in patterning a spatial region of slightly larger thickness on the top surface of the microcavity spacer layer, and growing the top Bragg mirror afterwards. To a larger thickness corresponds a lower frequency of the optical resonance. The spatial pattern then acts as a two-dimensional confining potential for the photon mode. The barriers of this potential can be made very shallow by introducing small thickness variations. This gives rise to both spatially confined modes and a continuum of ex-

tended modes at energies above the barrier. As a consequence of the linear exciton- photon coupling, the polaritons resulting from the strong coupling of these photon modes with the quantum well exciton, will also be characterized by a mixed spectrum containing both confined and extended states. In addition to an easier fabrication approach, this kind of structure presents considerable advantages with respect to micropillars,[10] where photon confinement is obtained by etching the whole cavity body, thus resulting exclusively in confined modes. Furthermore, the quantum well and most of the photonic structure are not etched, thus preserving the quality factor of the original planar cavity.

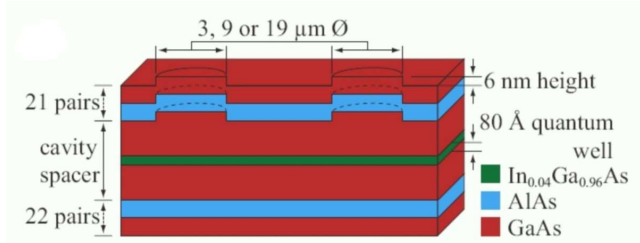


FIG. 1: Sketch of the sample (cross-section view). For clarity, the various lengths are not represented to scale.

The sample under investigation[18] is sketched in Fig 1. It is a semiconductor MC consisting of a  $\lambda$ -thick GaAs spacer layer sandwiched between AlAs/GaAs distributed Bragg reflectors made of a 21 (top) and 22 (bottom) double  $\lambda/4$ -layers. Embedded at the MC center is a single 8 nm  $\text{In}_{0.04}\text{Ga}_{0.96}\text{As}$  quantum well, characterized by a sharp exciton resonance at 1.484 eV. A slight wedge of 2.4 meV/mm of the microcavity wafer allows varying the cavity detuning across the exciton resonance. Before growing the top mirror, a pattern of 6 nm height has been chemically etched on the cavity spacer using a photolithography mask. The pattern shape and height is preserved throughout the growth up to the Bragg mirror top surface. Circular mesas with nominal diameter of 3, 9 and 19  $\mu\text{m}$  were patterned. The mesas are regularly spaced along the direction of the cavity wedge, so that mesas with varying exciton-cavity detuning for the laterally confined photon modes could be achieved. All our investigations were carried out at a temperature of 4 K, and consisted in PL measurements in the linear regime under pulsed off-resonance excitation at 760 nm, within the exciton continuum band. The sample was placed in the focal plane of a microscope objective. The excitation spot cross section had a Gaussian profile with 3  $\mu\text{m}$  extension allowing investigation of a single mesa. The angular emission pattern is contained on the Fourier plane behind the objective, and is imaged onto the entrance slit of a monochromator. The slit selects a narrow stripe across the center of the Fourier plane, which is then dispersed inside the monochromator and detected by a CCD

camera. In this way, thanks to the cylindrical symmetry, the spectral pattern of the emitted light, as a function of the energy and the emission angle, is directly displayed by the CCD.

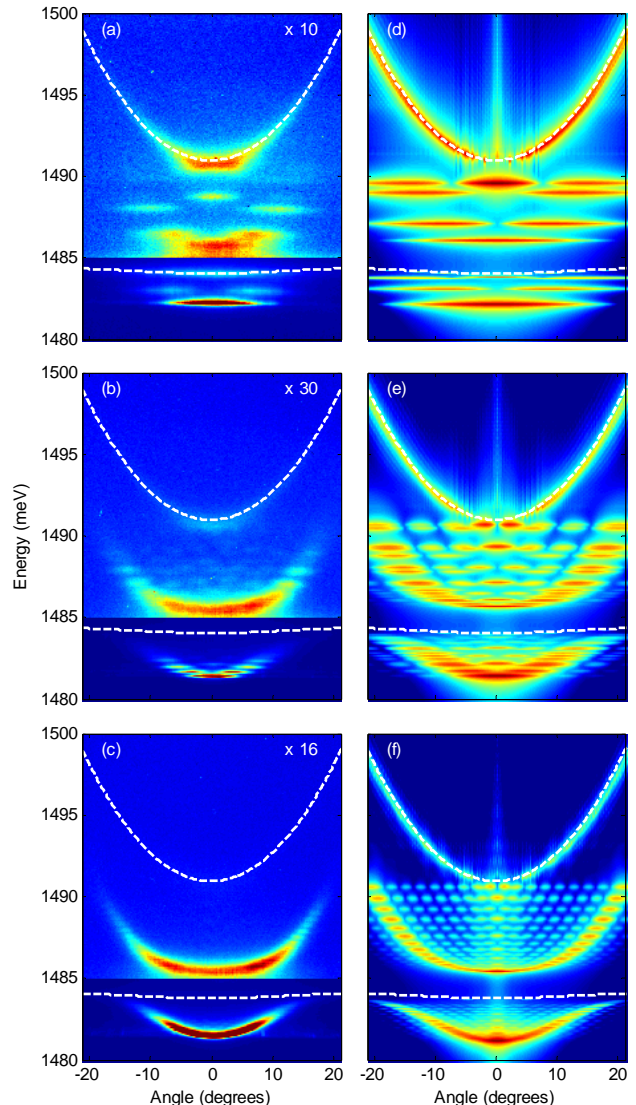


FIG. 2: Left: Measured polariton PL intensity (linear color scale from blue to red) as a function of energy and emission angle for the 3  $\mu\text{m}$  (a), 9  $\mu\text{m}$  (b) and 19  $\mu\text{m}$  (c) mesa. For clarity, the intensity above 1485 meV is multiplied by a constant factor, as indicated. Dashed: dispersion of the extended polariton modes, computed from a coupled oscillator model. Right: Intensity plot of the simulated polariton spectral density for the 3  $\mu\text{m}$  (d), 9  $\mu\text{m}$  (e) and 19  $\mu\text{m}$  (f) mesa (color log-scale, 4 decades from blue to red).

A polariton state laterally confined in a small circular mesa is expected to emit light in a broad pattern of angular directions, which directly relates to the polariton wave function in momentum space. We take advantage of this feature for the characterization of lateral confinement. The measured vacuum field Rabi splitting, at un-

processed regions far away from the mesas, is 3.8 meV, whereas the extrapolated linewidths are 200 and 500  $\mu\text{eV}$  respectively for the bare cavity mode and for the exciton. Large patterned regions (250  $\mu\text{m}$ ) fabricated for testing purposes[18] reveal a similar polariton dispersion with a cavity mode energy 9 meV lower than in the unprocessed regions. This value is consistent with a 6 nm thickness variation from mesa to barrier, as indicated by a transfer matrix calculation of the microcavity resonance.[8] When the excitation spot is focused on one mesa, the PL spectrum shows discrete narrow lines, in addition to a weak signature of the extended polariton states identical to that measured in the unprocessed regions of the sample. The dispersion pattern measured for 3, 9 and 19  $\mu\text{m}$  diameter mesas are displayed in Fig. 2 (a)-(c) respectively. The dispersion of the extended polariton (barely visible in the 19  $\mu\text{m}$  mesa) is highlighted by dashed lines in the plots. From this part of the dispersion we can infer a positive detuning of 6.4 meV between the extended cavity mode and the exciton. The strongest spectral features in the three images appear below and above the lower extended polariton mode. In particular, the 3  $\mu\text{m}$  mesa shows few discrete lines extending over broad angular regions, with energy spacings in the meV range. The 9  $\mu\text{m}$  mesa shows a larger number of more closely spaced spectral lines, with a smaller angular spread. Finally, in the 19  $\mu\text{m}$  mesa these features approach a quasi continuous spectrum, while the angular spread is still smaller.

This general trend, consisting in a narrowing of the angular emission pattern at fixed energy and a decrease of the energy spacing as the mesa diameter increases, is observed for any value of the exciton-cavity detuning. Spatial confinement explains in a natural way these observations. Indeed, confinement induces a discrete energy spectrum and localization of the wave functions in real space, which in turn produces extended features in reciprocal space explaining the angular spread observed in the emission. The mesas therefore act like spatial traps. Are these confined states polaritons, namely linear superposition of exciton and cavity photons? For extended polaritons, the evidence of this strong coupling regime is usually given by the level anticrossing between the two branches in the energy-momentum dispersion. For confined states, the discrete energy spectrum makes level anticrossing more difficult to characterize. In the case of the 9 and 19  $\mu\text{m}$  mesas in Fig. 2 (b) and (c), however, the discrete levels form a pattern displaying a distinct level anticrossing at approximately 15 degrees, with a vacuum field Rabi splitting close to the 3.8 meV measured for the extended polaritons. This is a clear proof of strong coupling. For the 3  $\mu\text{m}$  mesa, this feature is more difficult to characterize. However, we remark that in Fig. 2(a) the two levels at 1482.5 and 1483 meV, thus below the bare exciton energy, display the same angular pattern as the two levels lying above the bare exciton energy at 1485.5 and 1486 meV. This clearly gives evidence to the fact that

they are respectively lower and upper confined polariton states. This analysis proves that the strong coupling is preserved by spatial confinement and the species emitting are indeed mixed exciton-photon modes.

In order to support this interpretation, we compare the measured spectra to the prediction of a theoretical model.[19] The model consists in solving Maxwell equations inside the cavity, by making the assumption that the electromagnetic modes can be expressed as  $\mathbf{E}(\mathbf{r}) = \mathbf{E}(\boldsymbol{\rho}) \exp(ik_z(\boldsymbol{\rho})z)$ , namely by those of a locally planar Fabry-Pérot resonator. This ansatz is justified by the small thickness variation and the large lateral extension of the mesas, as compared to the wavelength. The resulting photon modes are then included in a linear exciton-photon coupling Hamiltonian which is diagonalized. The mesas were assumed of circular shape and the nominal parameters of the samples were used for the calculations. Figs. 2 (d)-(f) display the simulated polariton spectral density for the three different mesas. The energy-momentum structure of the simulated spectra should be compared to the experimental counterpart, whereas the relative spectral intensities in the PL data bear additional information on the polariton state populations, that cannot be accounted for in the simulated spectral density. A slight discrepancy in the energies of the smallest mesa is probably due to its shape not perfectly circular. In general however, the model faithfully reproduces both the energy position and angular extension of the various spectral features. This brings the final proof that the mesa structures are efficient traps for microcavity polaritons.

The intensity emitted from each polariton level is proportional, among other factors, to the number of polariton quasiparticles occupying that level.[9] The measured data in Fig. 2 (a)-(c) clearly show that the polariton population builds up in the lowest lying energy levels, indicating a rather effective energy- relaxation mechanism towards the bottom of the trap. A preliminary analysis indicates a Boltzmann-like distribution with a temperature of about  $T = 20$  K. This can be traced back to the presence of a large density of spatially extended states at energies above the confined states. In particular, in the data displayed in Fig. 2 (a)-(c), the lower extended polariton branch (lower dashed line) is almost fully exciton-like, with a vanishing photon component that results in a very long radiative lifetime. These states act as a reservoir from which quasiparticles relax to the confined states at lower energy. The relaxation can take place through interaction with the thermal bath of phonons,[20] with free carriers,[21] or via mutual polariton interaction.[22] The broken translational symmetry of the confined system lifts the constraint of momentum conservation, thus enhancing the relaxation efficiency compared to the case of a planar microcavity.

We have investigated the behaviour of the system at increasing excitation intensity. In Fig. 3 (a) we repro-

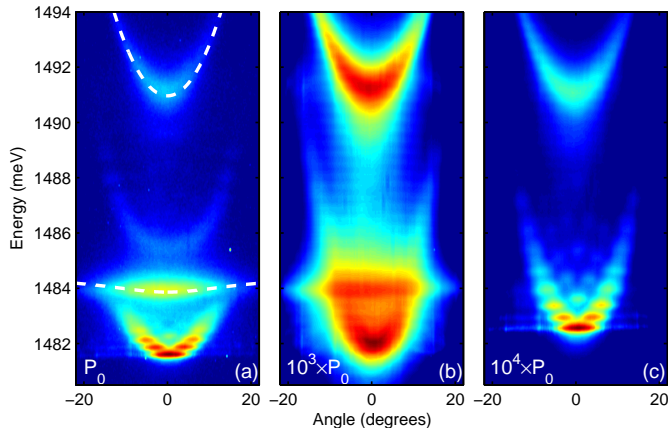


FIG. 3: (a) Measured PL intensity for the  $9 \mu\text{m}$  mesa at low pump intensity  $P_0$  in the linear regime (same data as in Fig. 2(b)). Dashed: extended polariton dispersion from a coupled oscillator model. (b) Pump intensity  $10^3 \times P_0$ . (c) Pump intensity  $10^4 \times P_0$ . Log-scale covering a factor 30 (a), 30 (b), and 100 (c) from blue to red.

duce the PL intensity in the linear emission regime (pump intensity  $P_0$ ) for the  $9 \mu\text{m}$  mesa. The log-scale allows to better display the different features of both confined and extended polaritons. In Fig. 3 (b) the pump intensity is 1000 times larger. Here, we observe a sizeable broadening of the spectral lines and the disappearing of strong coupling, displayed as a crossing (at  $\pm 13$  degrees) between the bare exciton dispersion the cavity-like dispersion of the mesa modes. Both features are expected as a result of the density-dependent oscillator strength saturation and the collisional broadening of the exciton transition.[23] At still higher pump intensity (Fig. 3 (c)) the bound exciton spectral signature vanishes, the lasing threshold is reached and sharp emission lines through the bare electromagnetic modes of the mesa structure appear. We point out that the linear regime of strongly-coupled polaritons is preserved in this sample over two decades of pump intensity. No evidence of final-state stimulation with macroscopic occupation of the ground polariton level was observed, presumably due to the low saturation density of this single-well GaAs-based sample in which exciton bleaching dominates over polariton bosonic stimulation.

The physics of the present system profoundly differs from the recently achieved strong coupling of a single quantum dot in a nano-resonator.[24, 25, 26] In that case, the strong coupling is a direct consequence of the three-dimensional photon confinement, and produces a single pair of mixed two-level states. Here, we produce zero-dimensional trapping of polariton quasi-particles which are already in the strong coupling regime in the absence of the lateral trap. As a consequence, several confined and extended polariton states coexist which, due to their bosonic nature, can be occupied by more than one exci-

tation quantum. All these features should help reaching the ideal situation of a weakly interacting cold Bose gas with a discrete energy spectrum, for which quantum collective phenomena are expected.[15] On the other hand, the shallow confining potential makes it possible to design structures with two or more resonant traps having a significant tunnelling probability. This, together with the ease in resonant spatially-resolved optical excitation and detection, and to the preparation of nonclassical states via parametric polariton scattering[13] can lead to a variety of easily accessible schemes for coherent manipulation of the polariton quantum phase, thus opening the way to applications in quantum information technology.

In conclusion, we have succeeded in tailoring semiconductor microcavities in a way allowing to obtain for the first time spatial trapping of polaritons. An angle-resolved PL study demonstrates the high quality of the trapping as well as the simultaneous presence of extended states at higher energy, resulting in enhanced energy relaxation efficiency. Polariton traps have the unique property of displaying zero-dimensional confinement of an electronic degree of freedom in a solid, already on the micron scale. This guarantees ease of fabrication, high reproducibility and on demand access to a variety of spectral features (e.g. by tailoring the mesa shape and size), thus holding great promise for the realization of integrated solid-state quantum micro-devices.

This work was supported by the Quantum Photonics NCCR and project N. 620-066060 of the Swiss National Research Foundation. We thank C. Ciuti, A. Quattropani and P. Schwendimann for helpful discussions. We are particularly grateful to W. Langbein for enlightening advice and H.-J. Bühlmann for technical help.

---

\* vincenzo.savona@epfl.ch

- [1] H. F. Hess, *et al.*, Science **264**, 1740 (1994).
- [2] A. P. Alivisatos, Science **271**, 933 (1996).
- [3] D. Bimberg, M. Grundmann, and N. N. Ledentsov, *Quantum Dot Heterostructures* (Wiley, New-York, 1999).
- [4] A. Hartmann, *et al.*, Phys. Rev. Lett. **84**, 5648 (2000).
- [5] E. Biolatti, R. C. Iotti, P. Zanardi, and F. Rossi, Phys. Rev. Lett. **85**, 5647 (2000).
- [6] C. Weisbuch, M. Nishioka, A. Ishikawa, and Y. Arakawa, Phys. Rev. Lett. **69**, 3314 (1992).
- [7] R. Houdré *et al.*, Phys. Rev. Lett. **73**, 2043 (1994).
- [8] V. Savona, L. C. Andreani, P. Schwendimann, and A. Quattropani, Solid State Commun. **93**, 733 (1995).
- [9] V. Savona *et al.*, Phys. Rev. B **53**, 13051 (1996).
- [10] G. Dasbach, M. Schwab, M. Bayer, and A. Forchel, Phys. Rev. B **64**, 201309 (2001).
- [11] R. M. Stevenson *et al.*, Phys. Rev. Lett. **85**, 3680 (2000).
- [12] W. Langbein, Phys. Rev. B **70**, 205301 (2004).
- [13] S. Savasta, O. D. Stefano, V. Savona, and W. Langbein, Phys. Rev. Lett. **94**, 246401 (2005).
- [14] J. Ph. Karr, A. Baas, R. Houdré, and E. Giacobino, Phys. Rev. A **69**, 031802 (2004).

- [15] J. Lauwers, A. Verbeure, and V. A. Zagrebnov, *J. Phys. A* **36**, L169 (2003).
- [16] D. Snoke, *Science* **298**, 1368 (2002).
- [17] V. Savona, and D. Sarchi, *phys. stat. sol. (b)* **242**, 2290 (2005).
- [18] O. El Daif *et al.*, *App. Phys. Lett.* **88**, 061105 (2006).
- [19] P. Lugan, D. Sarchi, and V. Savona, *cond-mat/0602628* (2006).
- [20] F. Tassone *et al.*, *Phys. Rev. B* **56**, 7554 (1997).
- [21] P. G. Lagoudakis *et al.*, *Phys. Rev. Lett.* **90**, 206401 (2003).
- [22] D. Porras, C. Ciuti, J. J. Baumberg, and C. Tejedor, *Phys. Rev. B* **66**, 085304 (2002).
- [23] G. Khitrova *et al.*, *Rev. Mod. Phys.* **71**, 1591 (1999).
- [24] J. P. Reithmaier *et al.*, *Nature* **432**, 197 (2004).
- [25] T. Yoshie *et al.*, *Nature* **432**, 200 (2004).
- [26] E. Peter *et al.*, *Phys. Rev. Lett.* **95**, 067401 (2005).